Structure of alkyl ammonium solutions in vermiculite clays

ARTICLE *in* FARADAY DISCUSSIONS · JANUARY 1996

Impact Factor: 4.61 · DOI: 10.1039/FD9960400295 · Source: OAI

Faraday Discuss., 1996, **104**, 295–306

Structure of alkyl ammonium solutions in vermiculite clays

Graham D. Williams,[a] Neal T. Skipper,*[a] Martin V. Smalley,[a] Alan K. Soper[b] and Steve M. King[b]

[a] *Department of Physics and Astronomy, University College, Gower St, London, UK WC1E 6BT*

[b] *ISIS Facility, Rutherford Appleton Laboratory, Chilton, Didcot, Oxon, UK OX11 0QZ*

Swelling vermiculite clays are ideal systems in which to study confined aqueous and organic fluids. The clay platelets themselves are well characterised and carry a negative charge of around 0.1–0.2 C m^{-2}. To balance this negative layer charge a variety of interlayer counterions can be exchanged into the clay pores. These counterions draw polar solvents, such as water, into the interlayer region, thereby forcing the clay platelets apart. We report on neutron diffraction studies of the hydration of vermiculites containing alkyl ammonium counterions. Owing to the subtle balance between hydrophobic and hydrophilic hydration these particular ions induce a fascinating variety of clay swelling behaviour. When the counterions are methyl or ethyl ammonium, vermiculites will only absorb a maximum of two layers of water. However, increasing the hydrophobic chain length can induce macroscopic colloidal swelling: in dilute aqueous solutions propyl and butyl ammonium vermiculites expand to form 1D colloidal gels, with layer spacings of up to 1000 Å. Surprisingly perhaps, this macroscopic swelling is not observed with slightly longer chain alkyl ammonium counterions, such as pentyl or hexyl. We find that the layer spacing in the macroscopically swollen gels is inversely proportional to the root of the salt concentration in the solution, and that there is a temperature-induced phase transition, in which the gels collapse at high temperatures. In both methyl and butyl ammonium vermiculite the counterions are only loosely bound to the clay platelets, and do not behave as surfactants. In the absence of any strong interlayer structuring we therefore attribute the macroscopic swelling of propyl and butyl ammonium vermiculites to the ability of the hydrophobic chains to weaken the clay–counterions–clay Coulombic attraction, without forming a water repellent micelle-like interlayer region.

1 Introduction

Swelling clay minerals such as vermiculites are ideal systems in which to study the properties of interfacial fluids. Vermiculites occur naturally as macroscopic (cm^3) crystals. These crystals are comprised of stacks of negatively charged mica-like sheets which are held together by charge-balancing interlayer counterions, such as sodium or calcium.[1] The interlayer counterions are fully exchangeable, and can be selected by soaking the crystal in an appropriate solution.

In addition to counterions, the interlayer region of vermiculites can also absorb a variety of solvent molecules, such as water or alcohols.[1] This process leads to expansion of vermiculites perpendicular to the plane of the clay layers, along the c^*-axis. Initially this expansion occurs in a series of discrete steps known as crystalline swelling.[1,2] Under certain thermodynamic conditions, and with certain interlayer counterions, crystalline swelling of vermiculites can be followed by the uptake of additional solvent.[1,3] This process is known as macroscopic or colloidal swelling.

An important example of macroscopic colloidal swelling occurs when vermiculite crystals containing certain alkyl ammonium counterions are immersed in water or dilute aqueous solutions.[3] In this case the clay crystals can absorb many times their own volume of water, to form a macroscopically swollen gel phase. These gels are characterised by a regular, controllable, layer spacing of up to 1000 Å. The transition from crystalline to gel phase is fully reversible, and there is no tendency for the clay layers to disperse beyond this spacing, indicating that the gel phase is in a true thermodynamic equilibrium. The gels therefore behave as ideal 1D colloids. As such, they provide a unique opportunity to measure solvent and counterion structure at a charged surface.[4–6] in the so-called electric double-layer, and to test theories of colloidal interactions.[7–11] Further interest stems from the many practical applications of alkyl ammonium ion substituted swelling clays, for example their ability to retard organic contaminants.[12]

We report on our neutron diffraction studies of vermiculites containing a series of alkyl ammonium counterions, from methyl to butyl ammonium. Macroscopic swelling of vermiculite crystals is observed in samples containing propyl and butyl ammonium counterions.[3] With these counterions the equilibrium clay layer spacing, d, can be controlled through the choice of external salt concentration, c: the layer spacing decreases with increasing concentration. The stability of the gel phase with respect to the crystal phase is affected by salt concentration, temperature and pressure. There is a c, T, P boundary between the two phases, the gel being favoured by low salt concentration, low temperature and high pressure.[10] Our work aims to quantify the structural and thermodynamic differences between these systems, and to clarify the mechanisms of colloidal swelling that lead to the gel–crystal phase transition. Small angle experiments are used to establish the T, c swelling behaviour of gel-phase crystals. Large-angle experiments, exploiting isotope substitution and difference analysis, are then used to measure the detailed interlayer structure in crystalline samples.

2 Samples and experimental methods

The vermiculite samples come from Eucatex in Brazil, and have the nominal composition:[1] $Si_{6.3}Mg_{5.44}Al_{1.65}Fe_{0.6}O_{20}(OH)_4 \cdot 1.3M^+ \cdot nH_2O$. The natural crystals were broken up into flakes of *ca.* 5 mm × 5 mm × 0.5 mm. They were soaked in 1 M NaCl solution, the solution being replaced every week, until the natural mixture of counterions was completely exchanged by sodium. They were then similarly exchanged in 1 M butyl ammonium chloride solution. Isotopically labelled samples and samples containing other alkyl ammonium ions were then prepared by exchanging these samples in an appropriate solution.

We are interested in the thermodynamic and structural properties of both crystalline and gel-phase alkyl ammonium vermiculite hydrates. We have therefore conducted both low-angle and high-angle neutron scattering studies of our samples. First, low-angle neutron diffraction has been used to determine the clay layer spacing and gel to crystal phase transition temperature for propyl and butyl ammonium substituted samples. Second, high-angle neutron diffraction has been used in conjunction with isotope substitution to determine the detailed interlayer structure in crystalline hydrated methyl and butyl ammonium vermiculites. We now describe briefly the methodologies of these two sets of experiments.

(i) Low-angle neutron diffraction

Experiments were carried out on the LOQ time-of-flight diffractometer at the ISIS pulsed-neutron source of the Rutherford Appleton Laboratory.[13,14] This instrument has a Q-range of 0.006–0.23 $Å^{-1}$, corresponding to d-spacings of 1000–25 Å. Neutron scattering intensity was measured *in situ* from vermiculite crystals contained in 1 cm × 1 cm

quartz cells and immersed in solutions of the counterion chloride. Samples were aligned with the clay layers horizontal and the scattering vector, $\boldsymbol{Q}$, parallel to the c^*-axis (Plate 1).

We have measured the layer spacing and the gel to crystal transition temperature as a function of salt concentration for both propyl and butyl ammonium counterions. The first three (00*l*) Bragg reflections were located at 4 °C, to find the layer spacing for each sample. The temperature was then increased in 2 °C steps, and the transition temperature from gel to crystal determined from the disappearance of the Bragg reflections. Fig. 1 illustrates a typical set of scattering patterns measured at four consecutive temperatures, and showing the gel–crystal phase transition between 313 and 311 K. At this point we note that body temperature is 311 K, and that similar temperature induced gel–crystal transitions are observed in many biochemical systems. An example is the deoxyhaemoglobin molecule that causes sickle cell anaemia.[15]

To assess sample to sample variations due to the small amounts of salt which become trapped within faults in the crystals, four samples were prepared for each concentration. Variation in layer spacing at a given external concentration is insignificant when the concentration in the soaking solution exceeds 0.1 M, but causes measurable variations in the clay layer spacing in more dilute solutions. The concentrations presented in Fig. 3 and 4 (later) therefore include a correction for the average salt trapped in the crystal, measured as 0.10 ± 0.05 M.[13]

(ii) High-angle neutron diffraction

Experiments were carried out on the LAD time-of-flight diffractometer at the ISIS pulsed-neutron source of the Rutherford Appleton Laboratory.[4–6] This instrument has

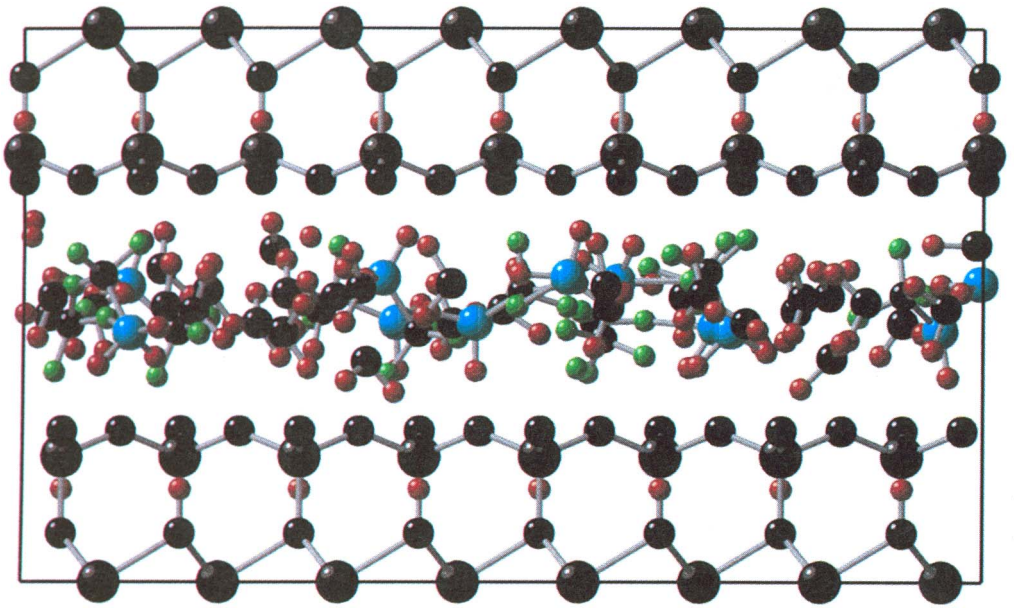

Plate 1 Molecular graphics snapshot of hydrated methyl ammonium vermiculite, with colour coding to show the species that we target by using isotopic substitution in conjunction with neutron diffraction (see Table 1). Red = hydrogen: blue = nitrogen: green = methyl: black = unsubstituted species (oxygen, magnesium, silicon and carbon). In the system illustrated the water content is 2.5 molecules per methyl ammonium counterion, and the clay layer spacing along the c^*-axis is 12.3 Å. During neutron diffraction experiments our samples were aligned so that the clay layers were perpendicular to the scattering vector, $\boldsymbol{Q}$.

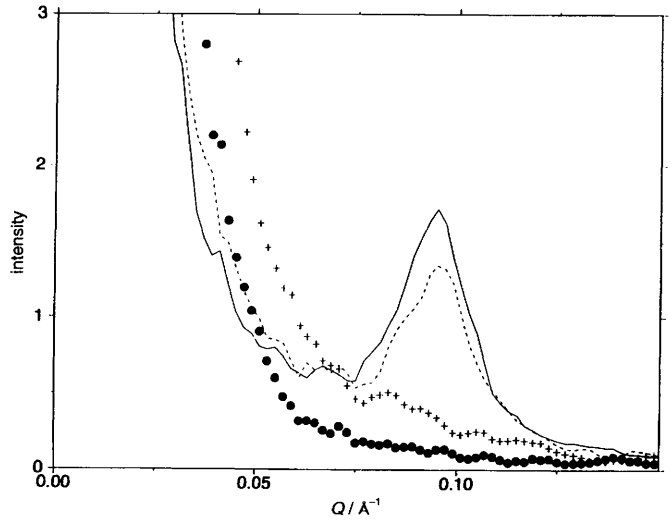

Fig. 1 Low-angle neutron scattering intensity as a function of scattering vector (Q/Å^{-1}) for propyl ammonium vermiculite immersed in 0.25 M propyl ammonium chloride solution. (——) 309, (— —) 311, (+) 313 and (●) 315 K. The low-angle peak at 0.1 Å^{-1} is due to a gel phase with a clay layer spacing of 60 Å. The data therefore show the temperature-induced gel–crystal phase transition occurring between 311 and 313 K. Note that body temperature is 311 K and that cell fluids are typically 0.25 M.

a Q-range of 0.2–0.50 Å^{-1}, corresponding to d-spacings of 25–0.12 Å. Neutron scattering intensity was measured *in situ* as a function of isotopic content from vermiculite crystals held between 0.3 mm thick vanadium sheets, and exposed to an atmosphere of 100% relative humidity. Samples were aligned with the scattering vector, $\boldsymbol{Q}$, parallel to

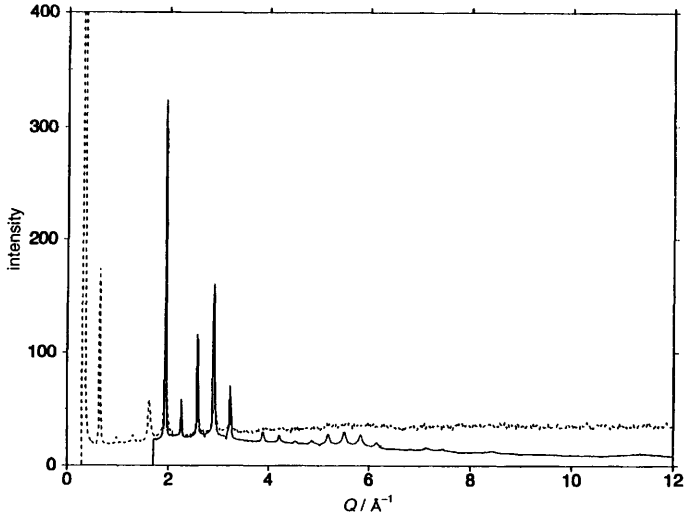

Fig. 2 High-angle neutron scattering intensity as a function of scattering vector (Q/Å^{-1}), for a fully hydrogenated butyl ammonium vermiculite crystal aligned with the c^*-axis parallel to the scattering vector. Overlapping plots are shown for scattering at $\theta = 10°$ (— —) and $\theta = 75°$ (——). From these data we can extract the intensities of the first 30 (00l) Bragg reflections. These intensities are used to calculate the density profiles in Fig. 5 [see eqn. (1)].

Table 1 Coherent neutron scattering lengths, b

nucleus	$b/10^{-14}$ m
^{1}H	−0.3374
^{2}H	0.6671
C	0.6651
^{15}N	0.937
^{14}N	0.644
O	0.5805
Mg	0.55
Al	0.345
Si	0.4107
Fe	0.993

the c^*-axis (Plate 1). Diffraction was measured at scattering angles of $\theta = 10° 75°$, allowing us to determine the intensities of the first 30 (00l) Bragg reflections (Fig. 2). The raw diffraction patterns were corrected for absorption and multiple scattering, and normalised by reference to the scattering from vanadium.[4] The integrated (00l) Bragg intensities, $I(Q)$, are then related to the neutron scattering density along the c^*-axis, $\rho(z)$, *via* the structure factor, $F(Q)$,

$$I(Q) = M(Q)|F(Q)|^2 \tag{1}$$

and

$$F(Q) = \int_{-d/2}^{d/2} \rho(z)\exp(iQz)\,dz \tag{2}$$

where d is the clay layer spacing, $M(Q)$ is a Q-dependent form factor which takes into account the effects of mosaic spread, finite sample size and the Debye–Waller factor.[4]

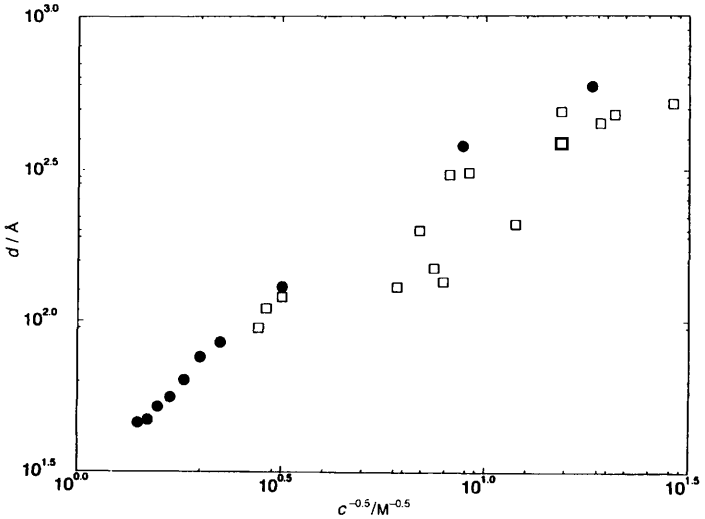

Fig. 3 Clay layer spacing (d) in vermiculite gels as a function of salt external concentration (c) for propyl (●) and butyl ammonium (□) vermiculite

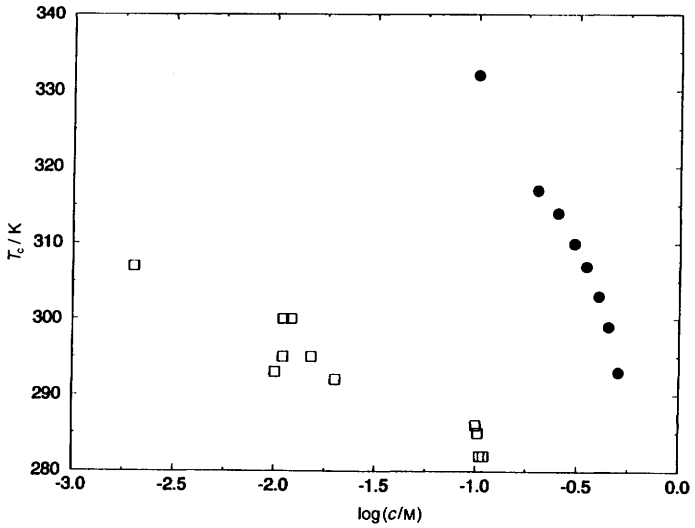

Fig. 4 Gel to crystal phase-transition temperature (T_c) in vermiculite as a function of salt concentration for propyl (●) and butyl ammonium (□) vermiculite

Neutron scattering density profiles, $\rho(z)$, were obtained from our scattering data by Monte Carlo fitting to the Bragg intensities.[4] *R*-factors for these fits are in the range 2–5%.

We have measured $F(Q)$ for crystalline hydrated methyl and butyl ammonium vermiculites with clay layer spacings of 12.3 and 19.4 Å, respectively. To improve the resolution of our data we have exploited isotope substitution among the interlayer counterions and water molecules. For each sample, four isotopically distinct samples were prepared, involving labelling of; water and ammonium protons (D for H), methyl protons (D for H) and ammonium nitrogen atoms (^{15}N for ^{nat}N). The scattering contrasts of these species are given in Table 1. Difference analysis of our scattering data then allows us to pick out the labelled species from the total scattering density.[4] Isotopically targeted species are colour coded in Plate 1, and density profiles are presented in Fig. 5 and 6 (later).

3 Results

(i) Low-angle neutron scattering from propyl and butyl ammonium vermiculite gels

The objectives of our low-angle neutron scattering experiments are to measure the clay layer spacings of colloidally swollen gel-phase vermiculites, as a function of salt concentration and temperature, and to identify the gel–crystal transition temperature. Fig. 3 shows the variation of the layer spacing, *d*, as a function of salt concentration, *c*, for propyl and butyl ammonium vermiculites immersed in dilute solutions. For both counterions, swelling does not occur at high salt concentrations. As the salt concentration is decreased a transition to the gel phase takes place. The concentration at which this occurs is 0.5 M for propyl ammonium vermiculite, which jumps from a spacing of 18.3 Å in the crystal to 45 Å in the gel, and 0.2 M for butyl ammonium vermiculite, which jumps from a spacing of 19.4 to 85 Å. As the concentration is further decreased, the clay layer spacing increases linearly with $c^{-0.5}$, the rate of change being 50 Å $M^{-0.5}$ for propyl compared with 25 Å $M^{-0.5}$ for butyl ammonium vermiculite. There is therefore a range of spacings between the crystal and the gel phase which cannot be obtained by controlling the salt concentration.

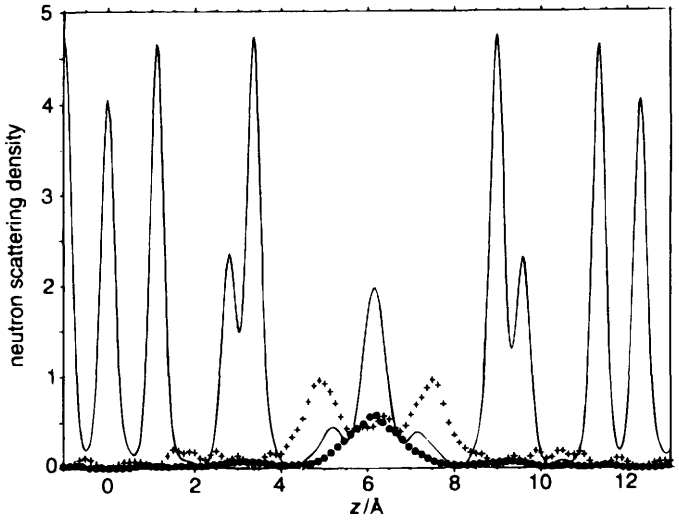

Fig. 5 Neutron scattering density profiles, $\rho(z)$, along the c^* clay stacking axis, for a hydrated methyl ammonium vermiculite crystal with a clay layer spacing of 12.3 Å (Table 2). Three profiles are shown, representing the scattering density due to the methyl group protons (●), the water and ammonium group protons (+), and all remaining atoms (——). A molecular graphics snapshot representation of this sample is shown in Plate 1.

Fig. 4 shows the gel to crystal phase-transition temperature, T_c, as a function of salt concentration for the same samples. With both counterions T_c decreases linearly with ln c. The rate of change of T_c is greater for propyl than for butyl ammonium; 50 K per log unit compared with 14.5 K per log unit, respectively, for polar solvents. Our results show that for propyl ammonium the phase transition to the gel occurs at higher temperatures

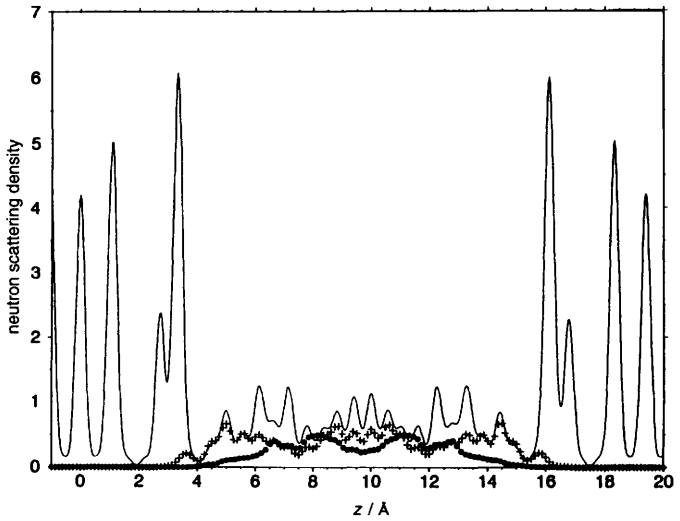

Fig. 6 Neutron scattering density profiles, $\rho(z)$, along the c^* clay stacking axis, for a hydrated butyl ammonium vermiculite crystal with a clay layer spacing of 19.8 Å (Table 3). Three profiles are shown, representing the scattering density due to the butyl group protons (●), the water and ammonium group protons (+) and all remaining atoms (——).

Table 2 Analysis of peaks in the fitted neutron scattering density profile, $\rho(z)$, for hydrated 12.3 Å methyl ammonium vermiculite[a] (Fig. 5)

z[b]	assignment	symbol	A[c]	chemical equivalent	
0.0	octahedral cations	line	59.5	5.44 Mg, 0.5 Fe	
1.0	oxygen	line	67.7	6.0 O[d]	clay
2.7	assignment	line	42.6	3.15 Si, 0.83 Al	layers
3.3	oxygen	line	67.7	6.0 O	
6.15	hydrogen (alkyl groups)	circles	35.1	3.1 H	interlayer
4.8	hydrogen (water and ammonium)	crosses	92.7	8.2 H	region
6.15	oxygen, nitrogen, carbon, hydrogen (alkyl groups)	line	54.6	1.3 $CH_3NH_3^+$, 4.1 O	

The water content of this sample is *ca.* 2.5 molecules per counterion. [a] Only peaks at or below 6.15 Å are listed. [b] Peak position (Å). [c] Peak area in arbitrary units. [d] Chemical equivalents are normalised by assuming the composition of this peak.

Table 3 Analysis of peaks in the fitted neutron scattering density profile, $\rho(z)$, for hydrated 19.4 Å butyl ammonium vermiculite[a] (Fig. 6)

z[b]	assignment	symbol	A[c]	chemical equivalent	
0.0	octahedral cations	line	62.4	5.44 Mg, 0.5 Fe	
1.0	oxygen	line	76.5	6.0 O[d]	clay
2.7	tetrahedral cations	line	45.5	3.15 Si, 0.83 Al	layers
3.3	oxygen	line	76.5	6.0 O	
8.2	hydrogen (alkyl groups)	circles	130.0	10.2 H	interlayer
5.5	hydrogen (water and ammonium)	crosses	200.0	15.7 H	region
9.7	oxygen, nitrogen, carbon, hydrogen (alkyl groups)	line	249.0	1.3 $C_4H_9NH_3^+$, (7.1 O)	

The water content of this sample is *ca.* 5.0 molecules per counterion. [a] Only peaks below 9.7 Å are listed. [b] Peak position (Å). [c] Peak area in arbitrary units. [d] Chemical equivalents are obtained by assuming the composition of this peak.

and higher concentrations than for butyl. The swelling of propyl ammonium vermiculites is also more rapid, occurring over minutes rather than hours. We currently have no results for the pressure dependence of swelling, except for butyl ammonium samples.[13]

(ii) High-angle neutron diffraction from crystalline hydrated methyl and butyl ammonium vermiculites

The objective of our high-angle neutron diffraction experiments is to measure the detailed interlayer structure in two hydrated vermiculites, one which exhibits macroscopic swelling and one which does not. We have, therefore, chosen to study samples containing butyl and methyl ammonium counterions.

Fig. 5 and 6 show the fitted density profiles for methyl and butyl ammonium, respectively. Because we have used isotopically labelled samples in conjunction with difference analysis, three profiles are shown in each case: the unsubstituted species, the exchangeable interlayer protons (on water and ammonium groups), and the alkyl group protons. We also obtained a separate profile for interlayer nitrogen, but this turned out to be featureless in our present samples. We are uncertain as to the reasons for this, but suspect that incomplete isotope substitution is the most likely cause. Table 1 gives the neutron scattering lengths for each species in the sample, including useful isotopes.

Tables 2 and 3 contain the intensities of the peaks in our density profiles, and the assignment of species to these peaks. In each case the scattering of substituted species is normalized to oxygen, so that number densities can be compared directly from our profiles. In each case clay layer peaks occur between 0.0 and 3.5 Å, with interlayer species beyond that. To obtain chemical equivalents we normalise to the peak at 1.0 Å, which is known to contain 6.0 oxygen atoms.[13] We now concentrate on the interlayer regions in our two sets of samples.

Our data for methyl ammonium vermiculite (Fig. 5) show a maximum in unsubstituted scattering density at 6.15 Å, which we attribute to the oxygen atoms of interlayer water molecules: we see from Table 1 that the overall contribution from alkyl groups is negative. The small shoulder at 5.1 Å is probably due to the nitrogen atoms of ammonium groups, but we have no significant nitrogen difference data to confirm this. Peaks in the substitutable hydrogen density are found at 4.9 and 7.4 Å. These positions are consistent with each water molecule forming hydrogen bonds to only one clay surface, as is the case in the single-layer hydrate of sodium vermiculite.[4] These proton peaks also contain the hydrogen atoms of ammonium groups. Alkyl group protons are located in a broad peak at 6.15 Å, completing the picture of a rather weakly structured interlayer region. This picture is confirmed by our preliminary Monte Carlo computer simulations of methyl ammonium vermiculite,[16,17] from which the snapshot in Plate 1 was taken.

Our data for butyl ammonium vermiculite point to an interlayer region that is, if anything, even less structured than that in methyl samples. From Fig. 6 we see unsubstituted density peaks at 5.0, 6.12, 7.14 and 9.44 Å, substitutable interlayer proton peaks at 4.94 and 8.86 Å, and an alkyl proton peak at 8.21 Å. Again, nitrogen substitution was unsuccessful, and resulted in a uniform distribution throughout the interlayer region. This sequence is consistent with rather weak hydrogen bonding of water to the clay surfaces, and a tendency for alkyl groups to occupy the centre of the interlayer region. However, we see no evidence for the formation of a micelle-like structure involving the hydrophobic chain groups, or strong bonding of the ammonium groups to the negatively charged clay surfaces.

4 Discussion

The swelling behaviour of alkyl ammonium vermiculites in aqueous solvents exhibits a fascinating variety as the hydrophobic chain length is increased. In particular, macro-

scopic swelling only occurs when the counterion is propyl or butyl ammonium.[3] Our current research aims to quantify the macroscopic swelling regime, and to provide structural insight into the temperature induced gel-crystal phase transition. Before we discuss our data for the vermiculites themselves, we first look at the thermodynamic solution properties of the alkyl ammonium ions in question.

If we consider the thermodynamics of the alkyl ammonium ions in solution there is little to suggest the rather subtle clay swelling behaviour we have observed. All the ions in the series up to hexyl ammonium exhibit almost ideal behaviour in solution. The enthalpies of solution of alkyl ammonium chloride salts in water have been measured.[18] In each case the enthalpy change on solvation is small, between -2.67 and $+12.7$ kJ mol^{-1}, and there is no systematic variation down the series. The solution of propyl ammonium chloride is slightly endothermic (1.38 kJ mol^{-1}) while for butyl ammonium it is slightly exothermic (-2.68 kJ mol^{-1}). We conclude that around propyl and butyl ammonium, the effects of hydrophobic and hydrophilic solvation are very finely balanced. The partial molar volumes of the ions have been measured,[19] and micelle formation is only seen in heptyl and octyl ammonium. It may, however, be possible that the confined geometry of the clays causes micelle formation in pentyl and hexyl ammonium ions. Future neutron diffraction experiments on aqueous solutions will examine the structural implications of this behaviour. We now turn to the hydration of alkyl ammonium vermiculites themselves.

The thermodynamics of the swelling process in butyl ammonium vermiculite has been measured.[19] The transition from crystal to gel is found to be exothermic, and accompanied by a decrease in entropy. Both the enthalpy and entropy changes are relatively small: between -5 and -10 J $[g(clay)]^{-1}$ depending on salt concentration, and between -0.02 and -0.04 J $[g(clay)]^{-1}$ K^{-1}, respectively. No equivalent measurements have been made for propyl ammonium vermiculite swelling. We conclude that the gel–crystal phase transition arises from a subtle balance between entropy and enthalpy. We therefore expect the transition to be sensitive to external conditions and alkyl chain length. In addition, since the hydration of the counterions is thermodynamically quite neutral, we anticipate that the swelling behaviour of the gel phase will be dominated by mean-field electrostatic interactions. These assertions are supported by our current data and by previous theoretical studies.[8–11]

We find that the interlayer region is relatively weakly structured in crystalline hydrates of both methyl and butyl ammonium vermiculites. This compares with the highly structured aqueous phases in sodium, lithium, calcium and nickel-substituted vermiculites.[4–6] We therefore propose that the limited hydration of methyl and ethyl ammonium samples is due to the weak interaction of these ions with water, which is unable to overcome the Coulombic clay–counterion–clay attraction. This attraction is weakened by increased hydrophobic chain length, which prizes the layers apart. Propyl and butyl ammonium ions are therefore able to induce macroscopic colloidal swelling. Presumably, if the alkyl chain length is increased further, the counterions begin to act as surfactants, with the central interlayer region repelling water. If this is the case, pentyl and hexyl ammonium vermiculites might exhibit colloidal swelling behaviour in non-aqueous solvents, such as alcohols.

5 Conclusion

We report on neutron diffraction studies of the swelling of alkyl ammonium vermiculites in aqueous solutions and water vapour. Owing to the subtle balance between hydrophobic and hydrophilic hydration these particular counterions induce a fascinating variety of clay swelling behaviour. When the counterions are methyl or ethyl ammonium, vermiculites will only absorb a maximum of two layers of water. However, increasing the hydrophobic chain length can induce macroscopic colloidal swelling: in dilute aqueous

solutions propyl and butyl ammonium vermiculites expand to form 1D colloidal gels, with layer spacings of up to 1000 Å. Surprisingly perhaps, this macroscopic swelling is not observed with slightly longer chain alkyl ammonium counterions, such as pentyl or hexyl. Our present research aims to establish the microscopic mechanisms underlying this pattern of swelling behaviour.

We have conducted low- and high-angle neutron diffraction experiments on vermiculites containing a series of alkyl ammonium counterions, from methyl to butyl ammonium. We find that the layer spacing in the macroscopically swollen gels is inversely proportional to the root of the salt concentration in the solution, and that there is a temperature-induced phase transition, in which the gels collapse at high temperatures. In both methyl and butyl ammonium vermiculite the counterions are only loosely bound to the clay platelets, and do not behave as surfactants. In the absence of any strong interlayer structuring we therefore attribute the macroscopic swelling of propyl and butyl ammonium vermiculites to the ability of the hydrophobic chains to weaken the clay–counterion–clay Coulombic attraction, without forming a water repellent micelle-like interlayer region. Future studies will investigate the hydration of alkyl ammonium ions in aqueous solutions, and vermiculite swelling in non-aqueous solvents.

References

1 A. C. D. Newman, *Chemistry of Clay and Clay Minerals*, Mineralogical Society, London, 1987.
2 J. A. Kittrick, *Soil Sci. Amer. Proc.*, 1969, **33**, 217.
3 W. G. Garrett and G. F. Walker, *Clays Clay Miner.*, 1962, **9**, 557.
4 N. T. Skipper, A. K. Soper and J. D. C. McConnell, *J. Chem. Phys.*, 1991, **94**, 5751.
5 N. T. Skipper, M. V. Smalley and A. K. Soper, *J. Phys. Chem.*, 1994, **98**, 942.
6 N. T. Skipper, M. V. Smalley, G. D. Williams, A. K. Soper, C. H. Thompson, *J. Phys. Chem.*, 1995, **99**, 14201.
7 R. Parsons, *Chem. Rev.*, 1990, **90**, 813.
8 I. Sogami and N. J. Ise, *Chem. Phys.*, 1984, **81**, 6320.
9 I. Sogami, T. Shinohara and M. V. Smalley, *Mol. Phys.*, 1991, **74**, 599.
10 K. S. Schmitz, *Acc. Chem. Res.*, 1996, **29**, 7.
11 N. Ise and Y. Hiroshi, *Acc. Chem. Res.*, 1996, **29**, 3.
12 S. A. Boyd, J-F. Lee and M. Mortland, *Nature (London)*, 1988, **333**, 345.
13 M. V. Smalley, R. K. Thomas, L. F. Braganza and T. Matsuo, *Clays Clay Miner.*, 1989, **37**, 474.
14 G. D. Williams, K. R. Moody, M. V. Smalley and S. M. King, *Clays Clay Miner.*, 1994, **42**, 614.
15 M. Murayama, *Science*, 1966, **153**, 145.
16 W. L. Jorgensen, J. D. Madura and C. J. Svenson, *J. Am. Chem. Soc.*, 1984, **106**, 6638.
17 E. S. Boek, P. V. Coveney and N. T. Skipper, *J. Am. Chem. Soc.*, 1995, **117**, 12608.
18 C. V. Krishnan and H. L. Friedman, *J. Phys. Chem.*, 1970, **74**, 3900.
19 S. Kurokawa, MSc Thesis, Osaka University, 1992.
20 J. E. Desnoyers and M. Arel, *Can. J. Chem.*, 1967, **45**, 359.

Paper 6/03928F; *Received 5th June*, 1996